Plasma Technology for Fuel Conversion

Min Suk Cha
King Abdullah University of Science and Technology (KAUST)
Physical Science and Engineering Division (PSE)/ Clean Combustion Research Center (CCRC)
4700 KAUST, Thuwal, 23955-6900, Saudi Arabia

ABSTRACT

Plasma-based fuel reforming is of interest area, since it can produce carbon-neutral fuels and may use carbon dioxide as feedstock. To better understand each effect of electron-induced chemistry and thermochemistry in plasma-assisted fuel reforming, we developed a temperature-controlled dielectric barrier discharge (DBD) reactor, which controlled the gas temperature and the electron temperature independently. The results of a partial oxidation, a dry reforming, and a steam reforming with methane have been reported, and, here, the trilogy was reviewed and summarized.

1. Introduction

Syngas, consists of mostly hydrogen and carbon monoxide, has been of interest topic since early 2000 driven by the hydrogen economy. The partial oxidation, the dry reforming, and the steam reforming are the major chemical processes to produce syngas. Nowadays, the dry reforming of methane, became popular since it utilizes carbon dioxide.

Plasma reforming processes, using corona discharge, dielectric barrier discharge (DBD), spark, gliding arc, and thermal arc, were extensively investigated. However, there are a lack of fundamental understanding for the plasma chemistry in the plasma reforming.

In our studies for the partial oxidation of methane, the dry reforming of methane, and the steam reforming of methane [1–3], we developed and introduced a temperature-controlled DBD reactor in which electron temperature and background temperature were controlled independently. Using this system, experimental studies were performed to elucidate the distinctive roles of the electron-induced chemistry and thermochemistry during the reforming processes.

As a result, we found the importance of the thermochemistry on product compositions, while the electron-induced chemistry could initiate the process even with very low temperature. Detailed review and comparison will be presented here.

2. Method

Fig. 1 Temperature controlled DBD reactor.

The experimental setup consisted of a temperature-controlled DBD reactor, a reactant feeding system, a high-voltage supply, and analytical systems. The temperature-controlled DBD reactor consisted of an electrically heated furnace and a DBD section made by a quartz tube installed inside the furnace. The quartz tube had a 630 mm long straight section with an inner diameter of 45 mm that allowed the gas mixture to reach a target temperature before the tube narrowed to accommodate the DBD section. A 45 mm long stainless-steel mesh serving as a ground electrode surrounded the narrow section of the quartz tube (20 mm inner and 25 mm outer diameter). A 17.5 mm thick stainless-steel circular rod was inserted into the center of the contracted quartz tube as a high-voltage electrode, forming a 1.25 mm gas gap between the rod electrode and the quartz tube.

A high-voltage supply (30/20 A, Trek) amplified a sinusoidal waveform from a function generator (AFG 3021B, Tektronix), whose amplitude and frequency could be adjusted, to operate the DBD. The voltages applied to the high-voltage electrode and across a sampling capacitor (10 nF), which was installed in the ground electrode to collect charges for the estimation of discharge power, were monitored by voltage probes (P6015A and TPP1000 Tektronix, respectively) with a digital oscilloscope (DPO 4140B, Tektronix). Five thousand cycles of the voltage waveforms were averaged for each tested condition to estimate the power.

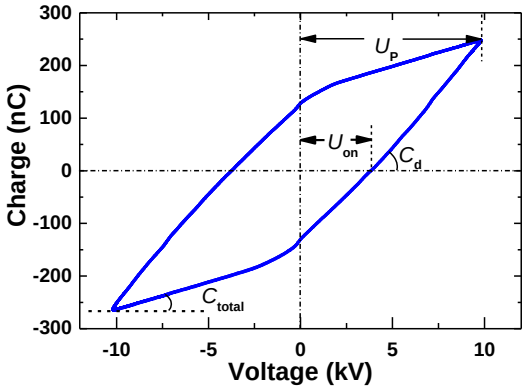

Fig. 2 A sample Lissajous diagram as in [3].

As indicated in Fig. 2, the Lissajous diagram was used to calculate the discharge power, P_{dis}, based on the

Corresponding author: Min Suk Cha
E-mail address: minsuk.cha@kaust.edu.sa

internal area of the parallelogram multiplied by the operating AC frequency, f_{ac}. An onset voltage (U_{on}) and the effective capacitances of the barrier (C_d) and a total system (C_{tot}) were also deduced from the Lissajous diagram and, as a consequence, the capacitance of the gas gap (C_g), the breakdown voltage (U_b) across the gas gap, and the reduced field intensity, E/N, were determined from $C_g = C_d C_{tot}/(C_d - C_{tot})$, $U_b = U_{on}/(1 + C_g/C_d)$, and $E/N \approx U_b/(dN)$, respectively, where d is the gas-gap distance in the DBD, N is the gas number density, and E is the averaged electric field in the gas gap.

3. Results and Discussion

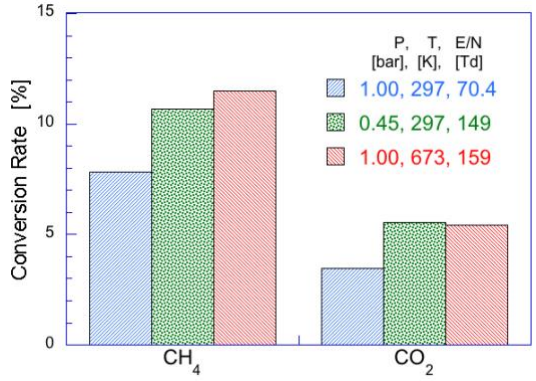

Fig. 3 Conversion of CH_4 and CO_2 in [1].

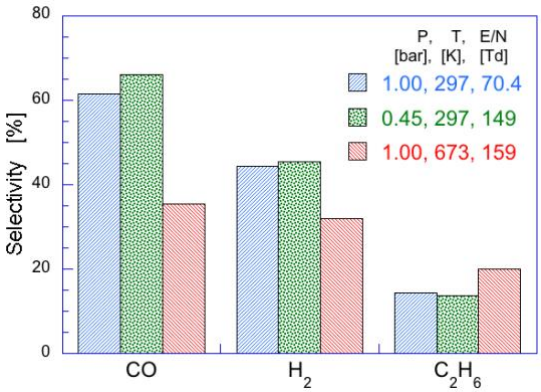

Fig. 4 Selectivity of CO, H_2, and C_2H_6 in [1].

Figures 3 and 4 show the conversion of reactant—methane and carbon dioxide—and the selectivities of product—hydrogen, carbon monoxide, and ethane—for the dry reforming of methane as in [1]. Since a gas density was varied as the background temperature varied, a reduced field intensity, which determines the electron temperature, was also affected. Thus, we add another test condition with varying pressure while the temperature maintains as a room temperature. As a result, the conversions of reactant were affected by E/N only (Fig. 3), indicating electron impact reactions are the most effective mechanism to decompose methane and carbon dioxide. On the other hand, the product distribution seems to be controlled by the background temperature (Fig. 4), irrespective of pressure and the reduced field intensity, which implies that, once the reaction is initiated by the electron impact reactions, the rest of chemical pathways to the product is determined by the background temperature.

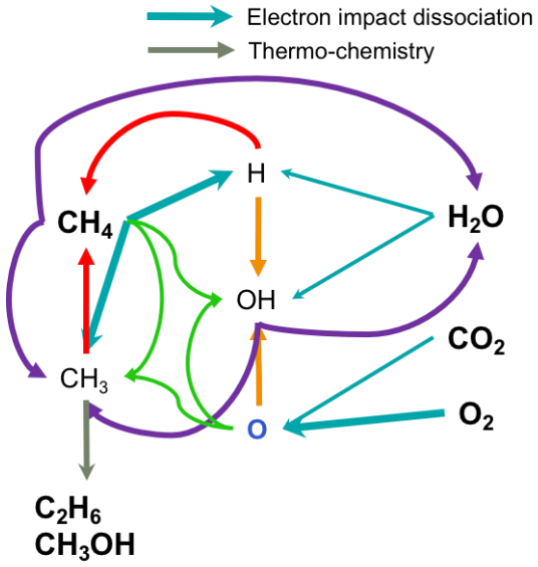

Fig. 5 Schematic of plasma chemistry with methane.

Figure 5 shows schematic chemical pathways combining three previous works [1–3]. The electron impact reactions can decompose CH_4 into CH_3 and H, create H and OH radicals from H_2O, and produce O radicals from O_2 and CO_2. Now, depending on the concentration of those radical pools, overall conversion of methane and product distribution are affected. For example, when increase OH concentration by adding H_2O, we can selectively increase the methanol formation.

4. Concluding Remarks

Temperature and pressure dependent data are available for modelers. Future efforts should be on the below area.

- Chemical kinetic model development and validation for the reforming reactions.
- Experiment and modeling to higher HCs to expand the knowledge into plasma assisted combustion as well as a fuel formulation.
- Detailed measurements for electric field, electron density, and spatially and temporally resolved species.

References

[1] X. Zhang, M.S. Cha, *J. Phys. D: Applied Phys.*, 46, (2013), 415205.

[2] X. Zhang, M.S. Cha, *Proc. Combust. Inst.*, 35, (2015), 3447-3454.

[3] J.-L. Liu, R. Snoeckx, M.S. Cha, *J. Phys. D: Applied Phys.*, 51, (2018), 385201.